HHS Public Access

Author manuscript

Biosens Bioelectron. Author manuscript; available in PMC 2016 November 09.

Published in final edited form as:

Biosens Bioelectron. 2015 September 15; 71: 269–277. doi:10.1016/j.bios.2015.04.044.

Electronic platform for real-time multi-parametric analysis of cellular behavior post-exposure to single-walled carbon nanotubes

Reem Eldawud[a], **Alixandra Wagner**[a], **Chenbo Dong**[a], **Yon Rojansakul**[b], and **Cerasela Zoica Dinu**[a,b,*]

[a]Department of Chemical Engineering, West Virginia University, WV 26506, United States

[b]Department of Basic Pharmaceutical Sciences, West Virginia University, WV 26505, United States

Abstract

Single-walled carbon nanotubes (SWCNTs) implementation in a variety of biomedical applications from bioimaging, to controlled drug delivery and cellular-directed alignment for muscle myofiber fabrication, has raised awareness of their potential toxicity. Nanotubes structural aspects which resemble asbestos, as well as their ability to induce cyto and genotoxicity upon interaction with biological systems by generating reactive oxygen species or inducing membrane damage, just to name a few, have led to focused efforts aimed to assess associated risks prior their user implementation. In this study, we employed a non-invasive and real-time electric cell impedance sensing (ECIS) platform to monitor behavior of lung epithelial cells upon exposure to a library of SWCNTs with user-defined physicochemical properties. Using the natural sensitivity of the cells, we evaluated SWCNT-induced cellular changes in relation to cell attachment, cell–cell interactions and cell viability respectively. Our methods have the potential to lead to the development of standardized assays for risk assessment of other nanomaterials as well as risk differentiation based on the nanomaterials surface chemistry, purity and agglomeration state.

Keywords

Single-walled carbon nanotubes (SWCNTs); Cell-based sensing; Real-time analysis; Cell adhesion; Viability

1. Introduction

Nanomaterials implementation in a variety of fields from microelectronics (Ouyang et al., 2002), to photo-optics (Li and Zhang, 2009), aerospace (Baur and Silverman, 2007), energy (Frackowiak and Béguin, 2001), sensors (Merkoçi et al., 2005), bioimaging (Barone et al., 2005), and drug delivery (Bianco et al., 2005) has raised awareness of their occupational safety and health-posed issues (Barillet et al., 2010; Golin et al., 2013). Current available

*Corresponding author at: Department of Chemical Engineering, West Virginia University, Benjamin M. Statler College of Engineering and Mineral Resources, PO Box 6102, Morgantown, WV 26506, United States. Fax: +1 304 293 4139. cerasela-zoica.dinu@mail.wvu.edu (C. Zoica Dinu).

techniques to assess *in vitro* toxicity of nanomaterials such as silica (Clément et al., 2013), silver nanoparticles (Speranza et al., 2013), carbon- (Gui et al., 2011) or metal-oxide-based (Vittori Antisari et al., 2013) rely on the functionality, affinity and/or selectivity of a biological recognition elements (e.g., biosensor, antibodies, cellular membrane, organelles or DNA etc.) as well as the processing power and detection capabilities of micro and optoelectronics (Mulchandani and Bassi, 1995; Zhao et al., 2014). Such techniques record nanomaterial-induced changes to single or a population of cells (for instance generation of reactive oxygen species (ROS) following exposure to silver nanoparticles (Gliga et al., 2014) or changes in cellular viability and proliferation post-exposure to gold (Jain et al., 2014) or titanium dioxide (Jaeger et al., 2012) etc.) at discrete, user-controlled time points (e.g., 12, 24 or 48 h) and mainly through invasive, laborious and costly assays that require intensive and time-sensitive manipulation or handling of the samples (Kostarelos et al., 2007; Nowak et al., 2014).

Recently it was however found that some of these techniques are less applicable and reliable for assessing toxicity of carbon nanotubes (CNTs), fullerenes (C_{60}), carbon black (CB), or quantum dots (QD) (Dhawan and Sharma, 2010; Monteiro-Riviere et al., 2009). For instance, results showed that CNTs' high surface area, high adsorption capability, high catalytic activity and their characteristic optical properties could interfere with the reagents used for toxicity detection affecting their emission capability (Kroll et al., 2009; Monteiro-Riviere et al., 2009; Worle-Knirsch et al., 2006). Specifically, several studies showed that the suitability and accuracy of assays relying on catalytic and affinity biosensors such as tetrazolium salt and neutral red (Dhawan and Sharma, 2010) routinely used to evaluate cellular viability, become questionable due to the adsorption or binding affinity of the reagents onto the CNT surfaces (Kroll et al., 2009; Monteiro-Riviere et al., 2009; Worle-Knirsch et al., 2006). Such limitations in the current CNT-induced hazard assessments (Monteiro-Riviere et al., 2009) as well as the continuous development of different CNT forms and shapes with various functionalities and physicochemical properties (Dong et al., 2013a; Marcolongo et al., 2007) do not allow for high-throughput and efficient toxicity assessment to be standardized and thus lead to minimum regulations of such nanomaterials exposure limits (Rogers-Nieman and Dinu, 2014). Specifically, according to Occupational Safety and Health Administration (OSHA), CNT exposures currently fall under the category of "particles not otherwise regulated" at a limit concentration of 5 mg/m^3 particles (Erdely et al., 2013; Lee et al., 2010). If CNTs are to reach their full potential for biotechnological applications (Bianco et al., 2005), new and scalable methods that allow for accurate cyto and genotoxicity evaluations need to be developed and implemented. Further, such methods should also allow for real-time assessment, minimum false positives, risk analysis of a variety of concentrations of nanomaterial being used for exposure, as well as risk correlations based on the nanomaterial length (Sato et al., 2005), diameter (Nagai et al., 2011), aggregation (Wick et al., 2007), impurities content (Aldieri et al., 2013), and/or surface chemistry (Saxena et al., 2007), just to name a few.

In this study, we implemented a rapid, non-invasive, high throughput, real-time continuous monitoring platform to detect CNT-induced changes in the behavior of confluent model human lung epithelial cells regularly used to investigate toxicity of nanomaterials of carbon (Gliga et al., 2014; Rogers-Nieman and Dinu, 2014; Siegrist et al., 2014). Our approach

relied on an electric cell impedance sensing (ECIS) platform that used cells immobilized onto gold electrodes as a proxy to assess SWCNT-associated risk exposures as well as help perform risk analysis and risk differentiation based on the nanotubes' physicochemical properties. By relying on the natural resistivity of the cells and the restrictions in the current pathways as imposed by the cell plasma membrane, comprehensive and multi-parametric analysis of the cellular behavior, cell attachment and cell–cell interactions were provided. ECIS platform was previously employed to monitor cellular changes upon exposure to digitoxin (a cardiac glycoside with anti-cancer potential; (Eldawud et al., 2014), cytochalasin D (a cytoskeletal inhibitor) (Opp et al., 2009) or sodium arsenate (a toxin responsible for cell retraction and changes in cytoskeleton) (Xiao et al., 2002a), all under user-controlled conditions. Our experimental procedure does not only capitalize on bioengineering means to provide parallel analysis of the cellular behavior upon exposure to a library of CNTs, all with high-sensitivity, in real-time and with minimum sample invasion, but further overcomes the limitations and concerns associated with the CNT interactions with the biological sensing elements. Further, our analysis could be extended to evaluate toxicity of other nanomaterials in a high-throughput and non-invasive fashion thus extending the ability for standardizing nanomaterial risk evaluation.

2. Materials and methods

2.1. Formation of the single-walled carbon nanotubes (SWCNTs) library

Acid treated single-walled carbon nanotubes (SWCNTs) were obtained by liquid phase oxidation of commercial (i.e., pristine) SWCNTs purchased from Unidym Inc. Specifically, the pristine SWCNTs were treated in a mixture of 3:1 (V/V) concentrated sulfuric (Fisher Scientific, 96.4%) and nitric (Fisher Scientific, 69.6%) acids for either 3 or 6 h to obtain SWCNTs with different degree of O-related functionalities and lengths (Campbell et al., 2013; Dong et al., 2013b). Upon time elapse, the SWCNTs/acids mixture was diluted in deionized water, filtered through a GTTP filter membrane (0.2 μm, Fisher Scientific) and washed extensively with deionized water to remove impurities or dissociated metal catalysts.

2.2. Characterization of the SWCNTs library

Raman spectroscopy was used to investigate the physical and chemical properties of the SWCNTs. For this, SWCNT powders (pristine or acid treated SWCNTs, both 3 and 6 h were assessed) were deposited onto clean glass slides and scanned using a Raman spectrometer (CL532-100, 100 mW, USA) and a 532 nm green laser with a spot size of $<0.01\ mm^2$ directed though a 50X objective. Detailed scans were recorded in the 100 to 3200 cm^{-1} range; low energy laser (i.e.,<0.5 mV) and short exposure time (i.e., 10 s) were maintained throughout data acquisition to prevent unexpected heating effects of the samples.

Energy dispersive X-ray spectroscopy (EDX) was employed for quantitative elemental analysis of the SWCNTs. Dry samples (pristine and acid treated SWCNTs) were mounted onto carbon tape and their elemental composition was evaluated using a Hi-tachi S-4700 Field Emission Scanning Electron Microscope with a S-4700 secondary detector and backscattered electron detector (in a single unit).

Atomic Force Microscopy (AFM) was used in air tapping mode to investigate the lengths of pristine and acid treated SWCNTs (Dong et al., 2013a; Marshall et al., 2006). Briefly, commercial Si tips (Asylum Research, AC240TS) were employed under their original manufacturing resonance frequency varying from 50 to 90 kHz. During the scanning process, the topography, phase and amplitude images of the SWCNT samples were collected simultaneously; a minimum of 3 scans were obtained for each SWCNTs sample being investigated and at least 30 individual SWCNTs were measured for an average of their length distribution.

Analysis of SWCNTs agglomeration state was performed using a dynamic light scattering device (DLS, Delsa Nano-Particle Analyzer, Beckman Coulter) that evaluated the dynamic fluctuations in the intensity of the scattered light as caused by the particles' Brownian motion (Cheng et al., 2011; Schwyzer et al., 2013, 2012). For this, suspensions of 50 μg/ml pristine and acid treated SWCNTs (both 3 and 6 h) were prepared in Dulbacco Minimum Essential Media (DMEM, Invitrogen) with 5% Fetal Bovine Serum (FBS, Invitrogen) and analyzed at 20 °C. For each sample, 150 measurements were recorded and the mean particle diameter was calculated using Stokes–Einstein relationship based on Photon Correlation Spectroscopy and it was corrected by analyzing the intensity, volume, and number distribution data collected for each samples using analytical software Delsa Nanoversion 2.21/ 2.03.

2.3. Cell culture and cell exposure to the SWCNTs library

Immortalized human lung epithelial cells (BEAS-2B) purchased from American Type Culture Collection (ATCC) were cultured in DMEM medium supplemented with 5% FBS, 2 mM L-glutamine and 100 units/ml penicillin/streptomycin (Invitrogen). Cells were passaged regularly and kept in 5% CO_2 at 37 °C. To prepare the pristine and acid treated SWCNTs (both 3 and 6 h) for cellular exposures, the samples were first dispersed by sonication in deionized water to eliminate all large agglomerates (visual assessment). Subsequently, the samples were filtered using a 0.2 μm pore filter membrane, resuspended in DMEM media with 5% FBS, and again sonicated for 2 min to form stable suspensions.

2.4. Electric cell impedance sensing (ECIS)

Real-time analysis of cellular behavior post-exposure to SWCNTs (pristine and acid treated, both 3 and 6 h) was performed using an electric cell impedance sensing (ECIS, Applied Biophysics) platform. In one set of experiments, two 8W10E+ ECIS arrays with 40 gold electrodes each were simultaneously employed to provide concomitant measurements of 16 samples, all at multiple frequencies. Prior to each experiment, the gold electrodes were pre-equilibrated and stabilized for 3 h with 400 μl of cellular media. Subsequently, BEAS-2B cells were seeded at a density of 2.5×10^5 cells/ml into each well and allowed to settle and grow over the electrodes for 24 h. After 24 h, the cells were exposed to suspensions of 100, 50 and 25 μg/ml pristine and acid treated SWCNTs in cellular media and their behavior was continuously monitored for 48 h. Using a multi-frequency recording mode, the resistance due to the current passing in the spaces between the basal cell membrane and gold electrodes was recorded as the alpha parameter (Eldawud et al., 2014) to evaluate the cell adhesion

characteristics and cell–substrate interactions (Giaever and Keese, 1993; Tiruppathi et al., 1992).

2.5. Cell analysis

BEAS-2B cells were seeded overnight onto a 12-well plate at a density of 2.5×10^5 cells/ml and exposed to suspensions of 100, 50 and 25 μg/ml pristine or acid treated SWCNTs (both 3 and 6 h were used) in cellular media for 24 and 48 h respectively. Subsequently, the cells were incubated with 10 μg/ml of Hoechst 33342 (Molecular Probes) for 30 min at 37 °C and then analyzed using fluorescence microscopy (Leica Microsystems) to assess the percentage of intensely condensed chromatin and/or fragmented nuclei. The apoptotic percentage was calculated as the percentage of cells showing apoptotic nuclei over the total number of cells investigated, both per field of view being considered.

Cellular viability was investigated using Trypan Blue exclusion assay (Invitrogen). For this, BEAS-2B cells were seeded overnight onto a 12-well plate at a density of 2.5×10^5 cells/ml and exposed to 100, 50 and 25 μg/ml pristine or acid treated SWCNT samples for 24 and 48 h respectively. Subsequently, the cells were washed twice with Phosphate Buffer Saline (PBS, Invitrogen), collected, stained with 0.4% Trypan Blue dye at 1:1 volume ratio and counted using Countess™ Automated Cell Counter (Invitrogen).

2.6. Statistical analyzes

All results are presented as mean±standard deviation. Two-way analysis of variance (ANOVA) and unpaired two-tailed Student's *T*-test were performed using JMP 8.0 (SAS Institute) and SigmaPlot 10.0 (Systat Software Inc.). Live cell count and apoptosis experiments were performed at least 3 times. The apoptotic percentage was calculated from scoring the nuclear deformation from approximately 1000 nuclei from ten random fields for each sample, at every time point, for a total of at least 30 measurements per each sample being investigated. ECIS experiments were performed in duplicates and repeated at least 3 times, for a minimum of 6 replicates per each sample. Results are considered significant when $^{*}p<0.05$.

3. Results

3.1. Preparation and characterization of the single-walled carbon nanotubes library

We prepared a library of single-walled carbon nanotubes (SWCNTs) with different physicochemical properties by using liquid phase oxidation of pristine SWCNTs in a strong mixture of nitric and sulfuric acids for 3 and 6 h respectively (Dong et al., 2013b; Wepasnick et al., 2011). The approach has been previously used to introduce O-containing functional groups (i.e., carboxyl, carbonyl groups), shorten the SWCNTs at the defect sites (Liu et al., 1998) and eliminate residual metal catalysts introduced during nanotube synthesis (Campbell et al., 2013; Dong et al., 2014).

Raman spectroscopy was used to characterize the structure, surface chemistry and degree of functionalization of the SWCNTs' library, all as a function of the acid treatment time (Fig. 1a). Results showed that the G band (1590 cm^{-1}), mainly associated with atomic

arrangement on the circumferential and axial direction of the SWCNT, did not undergo major changes upon acid treatment. In contrast, the D band (reflective of the sample disorder) became wider and shifted toward lower wavelengths, i.e., 1340.7 and 1338.1 for the 3 and 6 h treated SWCNTs both relative to 1353.50 cm^{-1} for pristine SWCNTs, suggesting that acid treatment altered the nanotubes surface chemistry and disrupted their well-structured walls. The intensity ratio between the D and G_{peaks} (I_D/I_G) for the 6 h treated SWCNTs was 0.47 ±0.056 relative to 0.253±0.048 for the pristine, and 0.21±0.102 for the 3 h treated SWCNTs respectively.

Energy dispersive X-ray spectroscopy (EDX; Fig. 1b) was used to characterize the elemental composition of the SWCNTs library before and after acid treatment. Analysis showed that acid treatment changed the composition of the SWCNTs by changing the percentage of O and C contents and reducing the percentage of metal impurities (i.e., Fe, Co, Cl), all as a function of the treatment period.

Analysis of the average length and agglomerate formation of pristine and acid treated SWCNTs were performed using an atomic force microscope (AFM) and dynamic light scattering respectively (Fig. 1c). Results showed that after 3 h acid treatment the average length of the pristine SWCNTs (844±162 nm) was reduced by 22% (656±207 nm), while 6 h acid treatment led to a 39% reduction (517±208 nm). Complementary, the average agglomerate size was reduced by 40% upon 3 h (from 615±133 to 378±83 nm) and by 22% (from 615±133 to 481±95 nm) upon 6 h acid treatment.

3.2. Real-time evaluation of the cellular behavior upon exposure to the SWCNTs' library

The effects of the SWCNTs' library on the behavior of model human lung epithelial cells (BEAS-2B) were assessed using electric cell impedance sensing (ECIS) and employing cells' natural sensitivity to provide high-throughput, parallel measurements of cellular attachment and cell–cell interactions (Giaever and Keese, 1993). Briefly, BEAS-2B cells were seeded onto the ECIS electrodes and exposed to 100, 50 and 25 μg/ml of either sample of SWCNTs being tested (namely pristine, 3 or 6 h treated) for 48 h. The doses chosen for this investigation were extrapolated from *in vivo* studies mimicking acute human exposure levels at Occupational Safety and Health Administration (OSHA) for particles less than 5 μm in diameter which correspond to workspace exposure at 5 mg/m^3 from 8 years up to a lifetime span (32 years) (Luanpitpong et al., 2014a; Sargent et al., 2012a).

Representative measurements of the resistance values of cells from the time of inoculation to the formation of a confluent monolayer, and subsequently post-exposure to pristine and acid treated SWCNTs are shown in Fig. 2. Results showed that upon cellular inoculation, the normalized resistance values increased in a time-dependent manner. This was shown to be due to the changes in the sensing area as determined by the interface between the cellular membrane and the gold electrode (Giaever and Keese, 1993; Tiruppathi et al., 1992). Specifically, if initially this interface was very small since when the cell reach/come into contact with the gold electrodes they have a near-spherical morphology, as the cells spread and grow onto the electrodes their shapes flatten leading to larger contact interfaces, with more attachment to the electrodes, and thus to an increase in the resistance value (Eldawud et al., 2014; Giaever and Keese, 1993; Xiao et al., 2002b) As the cells reached confluence,

minor fluctuations were recorded in the resistance values presumably due to the cellular micromotion onto the gold electrodes (Eldawud et al., 2014; Yashunsky et al., 2010) (Fig. 2a).

Upon exposure to the library of SWCNTs however, the resistance values exhibited significant changes in a manner dependent on the properties and doses of the SWCNTs being investigated. For instance, the resistance values for the cells exposed to pristine SWCNTs have dropped significantly to values lower than those of the control cells, however with no significant differences being observed for the different exposure doses being used (Fig. 2b). Cells exposed to 3 h treated SWCNTs showed a reduction in the resistance value relative to the control cells, with significant dose responses differences (Fig. 2c). Specifically, exposure to 100 μg/ml of the 3 h treated SWCNTs led to the highest drop in resistance; cells exposed to 50 and 25 μg/ml respectively showed smaller drops, all relative to controls. Cells exposed to 6 h treated SWCNTs also showed a drop in their resistance values relative to their control counterparts, all in a time and dose dependent manner; further, a gradual increase in the normalized resistance values was observed for the cells exposed for the 50 and 25 μg/ml exposure doses (Fig. 2d). Lastly, the analysis also showed that these cells were able to overcome the disturbance caused by the exposure and regained their resistance values within 48 h from the initial time of exposure.

Analyzes of the restrictions of the different current pathways passing through the spaces beneath the cellular monolayer and the gold electrodes were also performed as a function of the SWCNTs physicochemical characteristics. Specifically, analysis showed that alpha parameter, known to reflects cellular adhesion characteristics (Eldawud et al., 2014; Giaever and Keese, 1993), of the cells exposed to SWCNTs was significantly lower than that of the control cells, with the differences being dependent on both the type of the nanotube and the exposure dose being investigated. Specifically, while the cells exposed to pristine SWCNTs showed a small reduction (Fig. 3a), the cells exposed to 3 h treated SWCNTs showed a gradual decrease in their alpha which progressed both with time and the dose being tested (Fig. 3b). Finally, cells exposed to 6 h treated SWCNTs exhibited the highest reduction in alpha, all relative to controls, however with no differences being observed between the different doses being investigated (Fig. 3c).

Cross-comparison between the different subtypes in the SWCNT' library showed that exposure to the 6 h treated sample led to the highest dose-dependent reduction in cellular attachment relative to control cells and cells exposed to pristine and 3 h treated SWCNTs. The reductions were dose-dependent with 60%, 68% and 72% change observed for cells exposed to 25, 50 and 100 μg/ml SWCNTs respectively (Fig. 3d). Similarly, cellular exposure to 3 h treated SWCNTs led to 29%, 45% and 57% reduction in alpha after exposure to 25, 50 and 100 μg/ml nanotube respectively. In contrast, cells exposed to pristine SWCNTs showed the lowest reduction in the cellular attachment (about 10% less than the values of the control cells), with no significant differences being observed between the different exposure doses being investigated. Lastly, 48 h after exposure to 6 h treated SWCNTs, the cells were able to regain their adhesion characteristics with analysis revealing an average increase of about 38% of their alpha parameter relative to their alpha values after 24 h of exposure.

3.3. Analysis of cellular viability function of the SWCNT physicochemical properties

To test whether exposure to the SWCNTs' library affected cellular viability, we scored the number of cells showing changes in their nuclear morphologies as result of chromatin condensation or DNA fragmentation (Cui et al., 2005). Our results indicated that exposure to the SWCNTs induced a time and dose-dependent increase in the percentage of apoptotic cells (Fig. 4a) with cells exposed to pristine SWCNTs yielding about 12% and 16% apoptotic cells after 24 and 48 h respectively. Exposure to 3 h treated SWCNTs resulted in about 5% after 24 h and 11% apoptotic cells after 48 h, while exposure to 6 h treated SWCNTs resulted in about 7% after 24 h and 13% apoptotic cells after 48 h respectively.

Our analysis evaluating the number of live cells after 24 and 48 h exposure to the SWCNTs library complemented the results above (Fig. 4b) with examinations showing time, dose and SWCNT-properties dependent decrease in cellular viability of the exposed cells, all relative to controls. For instance, exposure to pristine, 3 and 6 h treated SWCNTs at 100 and 50 μg/ml doses showed a drop in the percentage of live cells of about 16%, 14% and 10%, with the decrease progressing to 30%, 22% and 18% respectively after 48 h of exposure, all relative to controls. Complimentary, 24 h exposure to 25 μg/ml of pristine, 3 and 6 h treated SWCNTs did not result in a significant reduction in the live cell counts, however 48 h exposure reduced the percentage of live cells by about 15%, 12% and 9% for the cells exposed to pristine, 3 and 6 h treated SWCNTs, all relative to control cells.

4. Discussion

Previous studies employing immunofluorescence (Sargent et al., 2009; Siegrist et al., 2014), flow cytometry (Dong et al., 2014), photospectroscopy (Monteiro-Riviere et al., 2009), or Western blotting (Lai et al., 2013) have provided insights into the nanotubes-induced toxicity after defined exposure periods. For instance, analysis showed that internalization of SWCNTs could activate different cellular mechanisms from ROS generation (Aldieri et al., 2013; Jaeger et al., 2012) to inflammation (van Berlo et al., 2014), cell signaling (Ellinger-Ziegelbauer and Pauluhn, 2009), protein expression (Lai et al., 2013), fibrogenesis (Muller et al., 2005; Porter et al., 2010), cellular attachment (Kaiser et al., 2013), viability (Cui et al., 2005) or proliferation (Müller et al., 2011), with such effects being dependent on the length (Manke et al., 2014; Sato et al., 2005), agglomeration (Wick et al., 2007), and surface chemistry (Jiang et al., 2009; Liu et al., 2014) of the nanotubes being tested. However, such methods failed to interpret intermediate exposure time points and mostly defined SWCNT-induced toxicity as invasive cellular changes reflected by cytoskeletal rearrangement (Umemoto et al., 2014), membrane disruption (Chang and Violi, 2006; Umemoto et al., 2014), disruption of the mitotic spindle (Sargent et al., 2012b) and cellular aneuploidy (Sargent et al., 2009; Siegrist et al., 2014), just to name a few.

Herein we provided a comprehensive, multi-parametric, non-invasive, high-throughput and real-time *in vitro* evaluation of the risk assessment upon exposure of model human lung epithelial cells to a library of SWCNTs. The library was prepared by incubation of pristine SWCNTs in a strong mixture of nitric and sulfuric acid for 3 and 6 h respectively (Dong et al., 2013a; Wepasnick et al., 2011). Raman, EDX and AFM cross-analyzes showed that acid treatment increased SWCNTs degree of functionalization with O-containing groups upon

cutting and oxidizing the nanotubes at their defect sites (Hu et al., 2003) and reduced their content of metal catalysts (i.e., Fe and Co) usually incorporated during manufacturing (Dong et al., 2013a). Measurements of the SWCNT agglomerates performed using DLS provided hydrodynamic diameter measurements of the nanotubes (Cheng et al., 2011; Schwyzer et al., 2013, 2012) and showed that smaller agglomerate size were obtained for the acid treated samples relative to pristine ones (Dong et al., 2013b; Jiang et al., 2009). The smaller agglomerate formation was further associated with the interplay between the Van der Waals attraction forces and the electrical repulsive forces caused by the O-rich groups present onto the individual sample according to the Schulze–Hardy rule (Desai et al., 2014; Sano et al., 2001).

Using ECIS high-throughput, real-time analysis we showed that changes in cellular behavior upon exposure to SWCNTs could be continuously and non-distractively monitored and related back to the dose and physicochemical characteristics (e.g., length, purity, hydrophilicity, and size of agglomerates) of the nanotubes being tested (Fig. 5). In particular, the multiple frequencies analysis assessing restrictions in the current pathways (Tiruppathi et al., 1992) helped classify changes in cell morphology as well as in the cell–cell/substrate interactions (Giaever and Keese, 1993) based on the library's characteristics. The analysis revealed that the increase in the O-groups led to higher SWCNTs' hydrophilicity which could presumably lead to their differential cellular internalization (Mu et al., 2009). A higher internalization could occur for the 6 h treated SWCNTs relative to both 3 h treated and pristine SWCNTs as reflected by the higher changes in both the resistance and cell adhesion properties. Based on the known interactions of the internalized nanotubes with the cytoskeletal elements, as well as cytoskeleton's role to regulate cell–substrate interactions (Holt et al., 2010; Umemoto et al., 2014), the regained adhesion characteristics observed after 48 h of exposure to 6 h treated SWCNTs could be associated with reduced cellular toxicity of these nanotubes. Complementary, changes in cellular adhesion could be associated with changes in cellular morphology (Song et al., 2013) and elasticity (Dong et al., 2014, 2013b), which in turn could influence cellular viability. Our analyzes of the percentage of apoptotic cells upon exposure to SWCNTs confirmed that nanotube's surface chemistry and degree of functionalization strongly influence cell viability in a time and dose dependent manner (Cui et al., 2005; Dong et al., 2013b; Patlolla et al., 2010; Ye et al., 2012). For instance, the higher reduction in cellular viability was observed for cells exposed to pristine SWCNTs which is presumably associated with the higher content of metal impurities, as well as the length and larger agglomerate size of these nanotubes relative to their acid treated counterparts.

Our results confirm previous studies which showed that exposure to longer SWCNTs induced increased toxic effects relative to shorter SWCNTs with exposure to longer nanotubes leading to an increase in the ROS generation (van Berlo et al., 2014), fibrosis (Luanpitpong et al., 2014b) and apoptosis (van Berlo et al., 2014), as well as reduction in cellular viability (Luanpitpong et al., 2014b; Manke et al., 2014). Further, our results confirm previous reports showing that the presence of metal impurities (i.e., Fe) in the nanotube samples resulted in higher cytotoxic and genotoxic effects (Aldieri et al., 2013), production of hydroxyl radicals, loss of intracellular low molecular weight thiols and accumulation of lipid hydroperoxides (Kagan et al., 2006), all by providing quantifiable

differential measurements on the cell–cell and cell–substrate interactions without prior cellular manipulation or labeling (Kaiser et al., 2013; Song et al., 2013).

5. Conclusions

Our study relied on the natural sensitivity of the cells used as primary transducers to provide real-time risk assessment of nanotube toxicity with minimum sample handling and sample invasion thus overcoming the limitations and concerns associated with SWCNT interactions with biological detection elements. Our results showed that human lung epithelial cells exposure to different doses of SWCNTs with user-defined physical and chemical properties leads to time and dose dependent changes in cellular behavior, adhesion properties and viability. In particular, results showed functional differences in the cellular behavior upon exposure to pristine and acid treated SWCNTs according to nanotube's length, surface chemistry, purity and agglomeration state thus helping extend the applications of the electric sensing platforms to help standardize nanomaterial risk evaluation.

Acknowledgments

Support for this work was through the National Science Foundation (NSF) Grants EPS-1003907 and 1434503, National Institute of Health (NIH; R01-ES022968), NanoSAFE and IGERT programs at West Virginia University (WVU). The authors further acknowledge use of WVU Shared Research Facilities, and the support and expertize of Dr. Karen Martin, the director of the Core Facility, as well as that of Dr. Jeremy Hardinger for the initial EDX analysis.

References

Aldieri E, Fenoglio I, Cesano F, Gazzano E, Gulino G, Scarano D, Attanasio A, Mazzucco G, Ghigo D, Fubini B. The role of iron impurities in the toxic effects exerted by short multiwalled carbon nanotubes (MWCNT) in murine alveolar macrophages. J Toxicol Environ Health (Part A). 2013; 76(18):1056–1071. [PubMed: 24188191]

Barillet S, Simon-Deckers A, Herlin-Boime N, Mayne-L'Hermite M, Reynaud C, Cassio D, Gouget B, Carriere M. Toxicological consequences of TiO_2, SiC nanoparticles and multi-walled carbon nanotubes exposure in several mammalian cell types: an in vitro study. J Nanopart Res. 2010; 12(1): 61–73.

Barone PW, Baik S, Heller DA, Strano MS. Near-infrared optical sensors based on single-walled carbon nanotubes. Nat Mater. 2005; 4(1):86–92. [PubMed: 15592477]

Baur J, Silverman E. Challenges and opportunities in multifunctional nanocomposite structures for aerospace applications. MRS Bull. 2007; 32(04):328–334.

Bianco A, Kostarelos K, Prato M. Applications of carbon nanotubes in drug delivery. Curr Opin Chem Biol. 2005; 9(6):674–679. [PubMed: 16233988]

Campbell AS, Dong C, Dordick JS, Dinu CZ. BioNano engineered hybrids for hypochlorous acid generation. Process Biochem. 2013; 48(9):1355–1360.

Chang R, Violi A. Insights into the effect of combustion-generated carbon nanoparticles on biological membranes: a computer simulation study. J Phys Chem B. 2006; 110(10):5073–5083. [PubMed: 16526750]

Cheng X, Zhong J, Meng J, Yang M, Jia F, Xu Z, Kong H, Xu H. Characterization of multiwalled carbon nanotubes dispersing in water and association with biological effects. J Nanomater. 2011; 2011:12.

Clément L, Zenerino A, Hurel C, Amigoni S, Taffin de Givenchy E, Guittard F, Marmier N. Toxicity assessment of silica nanoparticles, functionalised silica nanoparticles, and HASE-grafted silica nanoparticles. Sci Total Environ. 2013; 450–451:120–128.

Cui D, Tian F, Ozkan CS, Wang M, Gao H. Effect of single wall carbon nanotubes on human HEK293 cells. Toxicol Lett. 2005; 155(1):73–85. [PubMed: 15585362]

Desai C, Chen K, Mitra S. Aggregation behavior of nanodiamonds and their functionalized analogs in an aqueous environment. Environ Sci: Process Impacts. 2014; 16(3):518–523. [PubMed: 24352711]

Dhawan A, Sharma V. Toxicity assessment of nanomaterials: methods and challenges. Anal Bioanal Chem. 2010; 398(2):589–605. [PubMed: 20652549]

Dong C, Eldawud R, Sargent LM, Kashon ML, Lowry D, Rojanasakul Y, Dinu CZ. Towards elucidating the effects of purified MWCNTs on human lung epithelial cells. Environ Sci: Nano. 2014; 1(6):95–603. [PubMed: 25485116]

Dong C, Kashon ML, Lowry D, Dordick JS, Reynolds SH, Rojanasakul Y, Sargent LM, Dinu CZ. Exposure to carbon nanotubes leads to changes in the cellular biomechanics. Adv Healthc Mater. 2013a; 2(7):945–951. [PubMed: 23335423]

Dong CB, Campell AS, Eldawud R, Perhinschi G, Rojanasakul Y, Dinu CZ. Effects of acid treatment on structure, properties and biocompatibility of carbon nanotubes. Appl Surf Sci. 2013b; 264:261–268.

Eldawud R, Stueckle TA, Manivannan S, Elbaz H, Chen M, Rojanasakul Y, Dinu CZ. Real-time analysis of the effects of toxic, therapeutic and sub-therapeutic concentrations of digitoxin on lung cancer cells. Biosens Bioelectron. 2014; 59:192–199. [PubMed: 24727605]

Ellinger-Ziegelbauer H, Pauluhn J. Pulmonary toxicity of multi-walled carbon nanotubes (Baytubes®) relative to α-quartz following a single 6 h inhalation exposure of rats and a 3 months post-exposure period. Toxicology. 2009; 266(1–3):16–29. [PubMed: 19836432]

Erdely A, Dahm M, Chen B, Zeidler-Erdely P, Fernback J, Birch M, Evans D, Kashon M, Deddens J, Hulderman T. Carbon nanotube dosimetry: from workplace exposure assessment to inhalation toxicology. Part Fibre Toxicol. 2013; 10:53. [PubMed: 24144386]

Frackowiak E, Béguin F. Carbon materials for the electrochemical storage of energy in capacitors. Carbon. 2001; 39(6):937–950.

Giaever I, Keese CR. A morphological biosensor for mammalian cells. Nature. 1993; 366(6455):591–592. [PubMed: 8255299]

Gliga A, Skoglund S, Odnevall Wallinder I, Fadeel B, Karlsson H. Size-dependent cytotoxicity of silver nanoparticles in human lung cells: the role of cellular uptake, agglomeration and Ag release. Part Fibre Toxicol. 2014; 11(1):1–17. [PubMed: 24382024]

Golin CB, Bougher TL, Mallow A, Cola BA. Toward a comprehensive framework for nanomaterials: an interdisciplinary assessment of the current Environmental Health and Safety Regulation regarding the handling of carbon nanotubes. J Chem Health Saf. 2013; 20(4):9–24.

Gui S, Zhang Z, Zheng L, Cui Y, Liu X, Li N, Sang X, Sun Q, Gao G, Cheng Z, Wang L, Tang M, Hong F. Molecular mechanism of kidney injury of mice caused by exposure to titanium dioxide nanoparticles. J Hazard Mater. 2011; 195:365–370. [PubMed: 21907489]

Holt BD, Short PA, Rape AD, Wang YL, Islam MF, Dahl KN. Carbon nanotubes reorganize actin structures in cells and ex vivo. ACS Nano. 2010; 4(8):4872–4878. [PubMed: 20669976]

Hu H, Zhao B, Itkis ME, Haddon RC. Nitric acid purification of single-walled carbon nanotubes. J Phys Chem B. 2003; 107(50):13838–13842.

Jaeger A, Weiss DG, Jonas L, Kriehuber R. Oxidative stress-induced cytotoxic and genotoxic effects of nano-sized titanium dioxide particles in human HaCaT keratinocytes. Toxicology. 2012; 296(1–3): 27–36. [PubMed: 22449567]

Jain S, Coulter JA, Butterworth KT, Hounsell AR, McMahon SJ, Hyland WB, Muir MF, Dickson GR, Prise KM, Currell FJ, Hirst DG, O'Sullivan JM. Gold nanoparticle cellular uptake, toxicity and radiosensitisation in hypoxic conditions. Radiother Oncol. 2014; 110(2):342–347. [PubMed: 24444528]

Jiang J, Oberdörster G, Biswas P. Characterization of size, surface charge, and agglomeration state of nanoparticle dispersions for toxicological studies. J Nanopart Res. 2009; 11(1):77–89.

Kagan VE, Tyurina YY, Tyurin VA, Konduru NV, Potapovich AI, Osipov AN, Kisin ER, Schwegler-Berry D, Mercer R, Castranova V, Shvedova AA. Direct and indirect effects of single walled

carbon nanotubes on RAW 264.7 macrophages: role of iron. Toxicol Lett. 2006; 165(1):88–100. [PubMed: 16527436]

Kaiser JP, Buerki-Thurnherr T, Wick P. Influence of single walled carbon nanotubes at subtoxical concentrations on cell adhesion and other cell parameters of human epithelial cells. J King Saud Univ: Sci. 2013; 25(1):15–27.

Kostarelos K, Lacerda L, Pastorin G, Wu W, WieckowskiSebastien Luangsivilay, Godefroy S, Pantarotto D, Briand JP, Muller S, Prato M, Bianco A. Cellular uptake of functionalized carbon nanotubes is independent of functional group and cell type. Nat Nano. 2007; 2(2):108–113.

Kroll A, Pillukat MH, Hahn D, Schnekenburger J. Current in vitro methods in nanoparticle risk assessment: limitations and challenges. Eur J Pharm Biopharm. 2009; 72(2):370–377. [PubMed: 18775492]

Lai X, Blazer-Yost BL, Clack JW, Fears SL, Mitra S, Ntim SA, Ringham HN, Witzmann FA. Protein expression profiles of intestinal epithelial co-cultures: effect of functionalised carbon nanotube exposure. Int J Biomed Nanosci Nanotechnol. 2013; 3(1–2):054508.doi: 10.1504/IJBNN.2013

Lee J, Lee S, Bae G, Jeon K, Yoon J, Ji J, Sung J, Lee B, Yang J. Exposure assessment of carbon nanotube manufacturing workplaces. Inhal Toxicol. 2010; 22:369–381. [PubMed: 20121582]

Li J, Zhang JZ. Optical properties and applications of hybrid semiconductor nanomaterials. Coord Chem Rev. 2009; 253(23–24):3015–3041.

Liu J, Rinzler AG, Dai HJ, Hafner JH, Bradley RK, Boul PJ, Lu A, Iverson T, Shelimov K, Huffman CB, Rodriguez-Macias F, Shon YS, Lee TR, Colbert DT, Smalley RE. Fullerene pipes. Science. 1998; 280(5367):1253–1256. [PubMed: 9596576]

Liu ZB, Dong X, Song LP, Zhang HL, Liu LX, Zhu DW, Song CX, Leng XG. Carboxylation of multiwalled carbon nanotube enhanced its biocompatibility with L02 cells through decreased activation of mitochondrial apoptotic pathway. J Biomed Mater Res A. 2014; 102(3):665–673. [PubMed: 23554228]

Luanpitpong S, Wang L, Castranova V, Rojanasakul Y. Induction of stem-like cells with malignant properties by chronic exposure of human lung epithelial cells to single-walled carbon nanotubes. Part Fibre Toxicol. 2014a; 11(1):22. [PubMed: 24885671]

Luanpitpong S, Wang L, Manke A, Martin KH, Ammer AG, Castranova V, Yang Y, Rojansakul Y. Induction of stemlike cells with fibrogenic properties by carbon nanotubes and its role in fibrogenesis. Nano Lett. 2014b; 14(6):3110–3116. [PubMed: 24873662]

Manke A, Luanpitpong S, Dong C, Wang L, He X, Battelli L, Derk R, Stueckle T, Porter D, Sager T, Gou H, Dinu C, Wu N, Mercer R, Rojanasakul Y. Effect of fiber length on carbon nanotube-induced fibrogenesis. Int J Mol Sci. 2014; 15(5):7444–7461. [PubMed: 24786100]

Marcolongo G, Ruaro G, Gobbo M, Meneghetti M. Amino acid functionalization of double-wall carbon nanotubes studied by Raman spectroscopy. Chem Commun. 2007; 5:4925–4927.

Marshall MW, Popa-Nita S, Shapter JG. Measurement of functionalised carbon nanotube carboxylic acid groups using a simple chemical process. Carbon. 2006; 44(7):1137–1141.

Merkoçi A, Pumera M, Llopis X, Pérez B, del Valle M, Alegret S. New materials for electrochemical sensing VI: carbon nanotubes. TrAC Trends Anal Chem. 2005; 24(9):826–838.

Monteiro-Riviere NA, Inman AO, Zhang LW. Limitations and relative utility of screening assays to assess engineered nanoparticle toxicity in a human cell line. Toxicol Appl Pharmacol. 2009; 234(2):222–235. [PubMed: 18983864]

Mu Q, Broughton DL, Yan B. Endosomal leakage and nuclear translocation of multiwalled carbon nanotubes: developing a model for cell uptake. Nano Lett. 2009; 9(12):4370–4375. [PubMed: 19902917]

Mulchandani A, Bassi AS. Principles and applications of biosensors for bioprocess monitoring and control. Crit Rev Biotechnol. 1995; 15(2):105–124. [PubMed: 7641291]

Muller J, Huaux F, Moreau N, Misson P, Heilier JF, Delos M, Arras M, Fonseca A, Nagy JB, Lison D. Respiratory toxicity of multi-wall carbon nanotubes. Toxicol Appl Pharmacol. 2005; 207(3):221–231. [PubMed: 16129115]

Müller J, Thirion C, Pfaffl MW. Electric cell-substrate impedance sensing (ECIS) based real-time measurement of titer dependent cytotoxicity induced by adenoviral vectors in an IPI-2I cell culture model. Biosens Bioelectron. 2011; 26(5):2000–2005. [PubMed: 20875729]

Nagai H, Okazaki Y, Chew S, Misawa N, Yamashita Y, Akatsuka S, Ishihara T, Yamashita K, Yoshikawa Y, Yasui H. Diameter and rigidity of multi-walled carbon nanotubes are critical factors in mesothelial injury and carcinogenesis. Proc Natl Acad Sci USA. 2011; 108:E1330–E1338. [PubMed: 22084097]

Nowak J, Mehn D, Nativo P, Garcia C, Gioria S, Ojea-Jimenez I, Gilliland D, Rossi F. Silica nanoparticle uptake induces survival mechanism in A549 cells by the activation of autophagy but not apoptosis. Toxicol Lett. 2014; 224:84–92. [PubMed: 24140553]

Opp D, Wafula B, Lim J, Huang E, Lo JC, Lo CM. Use of electric cell–substrate impedance sensing to assess in vitro cytotoxicity. Biosens Bioelectron. 2009; 24(8):2625–2629. [PubMed: 19230649]

Ouyang M, Huang JL, Lieber CM. Fundamental electronic properties and applications of single-walled carbon nanotubes. Acc Chem Res. 2002; 35(12):1018–1025. [PubMed: 12484789]

Patlolla A, Knighten B, Tchounwou P. Multi-walled carbon nanotubes induce cytotoxicity, genotoxicity and apoptosis in normal human dermal fibroblast cells. Ethn Dis. 2010; 20(1 Suppl 1):S1-65–72.

Porter DW, Hubbs AF, Mercer RR, Wu NQ, Wolfarth MG, Sriram K, Leonard S, Battelli L, Schwegler-Berry D, Friend S, Andrew M, Chen BT, Tsuruoka S, Endo M, Castranova V. Mouse pulmonary dose- and time course-responses induced by exposure to multi-walled carbon nanotubes. Toxicology. 2010; 269(2–3):136–147. [PubMed: 19857541]

Rogers-Nieman GM, Dinu CZ. Therapeutic applications of carbon nanotubes: opportunities and challenges. Wiley Interdiscip Rev: Nanomed Nanobiotechnol. 2014; 6(4):327–337. [PubMed: 24715535]

Sano M, Okamura J, Shinkai S. Colloidal nature of single-walled carbon nanotubes in electrolyte solution: the Schulze–Hardy rule. Langmuir. 2001; 17(22):7172–7173.

Sargent L, Reynolds S, Lowry D, Kashon M, Benkovic S, Salisbury J, Hubbs A, Keane M, Mastovich J, Bunker K. Genotoxicity of multi-walled carbon nanotubes at occupationally relevant doses. Proc Am Assoc Cancer Res. 2012a; 53:1320.

Sargent LM, Hubbs AF, Young SH, Kashon ML, Dinu CZ, Salisbury JL, Benkovic SA, Lowry DT, Murray AR, Kisin ER, Siegrist KJ, Battelli L, Mastovich J, Sturgeon JL, Bunker KL, Shvedova AA, Reynolds SH. Single-walled carbon nanotube-induced mitotic disruption. Mutat Res. 2012b; 745(1–2):28–37. [PubMed: 22178868]

Sargent LM, Shvedova AA, Hubbs AF, Salisbury JL, Benkovic SA, Kashon ML, Lowry DT, Murray AR, Kisin ER, Friend S, McKinstry KT, Battelli L, Reynolds SH. Induction of aneuploidy by single-walled carbon nanotubes. Environ Mol Mutagen. 2009; 50(8):708–717. [PubMed: 19774611]

Sato Y, Yokoyama A, Shibata K, Akimoto Y, Ogino S, Nodasaka Y, Kohgo T, Tamura K, Akasaka T, Uo M, Motomiya K, Jeyadevan B, Ishiguro M, Hatakeyama R, Watari F, Tohji K. Influence of length on cytotoxicity of multi-walled carbon nanotubes against human acute monocytic leukemia cell line THP-1 in vitro and subcutaneous tissue of rats in vivo. Mol BioSyst. 2005; 1(2):176–182. [PubMed: 16880981]

Saxena RK, Williams W, McGee JK, Daniels MJ, Boykin E, Ian Gilmour M. Enhanced in vitro and in vivo toxicity of polydispersed acid-functionalized single-wall carbon nanotubes. Nanotoxicology. 2007; 1(4):291–300.

Schwyzer I, Kaegi R, Sigg L, Nowack B. Colloidal stability of suspended and agglomerate structures of settled carbon nanotubes in different aqueous matrices. Water Res. 2013; 47(12):3910–3920. [PubMed: 23582307]

Schwyzer I, Kaegi R, Sigg L, Smajda R, Magrez A, Nowack B. Long-term colloidal stability of 10 carbon nanotube types in the absence/presence of humic acid and calcium. Environ Pollut. 2012; 169(0):64–73. [PubMed: 22683482]

Siegrist K, Reynolds S, Kashon M, Lowry D, Dong C, Hubbs A, Young SH, Salisbury J, Porter D, Benkovic S, McCawley M, Keane M, Mastovich J, Bunker K, Cena L, Sparrow M, Sturgeon J, Dinu C, Sargent L. Genotoxicity of multi-walled carbon nanotubes at occupationally relevant doses. Part Fibre Toxicol. 2014; 11(1):6. [PubMed: 24479647]

Song M, Zeng L, Yuan S, Yin J, Wang H, Jiang G. Study of cytotoxic effects of single-walled carbon nanotubes functionalized with different chemical groups on human MCF7 cells. Chemosphere. 2013; 92(5):576–582. [PubMed: 23648328]

Speranza A, Crinelli R, Scoccianti V, Taddei AR, Iacobucci M, Bhattacharya P, Ke PC. In vitro toxicity of silver nanoparticles to kiwifruit pollen exhibits peculiar traits beyond the cause of silver ion release. Environ Pollut. 2013; 179:258–267. [PubMed: 23702492]

Tiruppathi C, Malik AB, Del Vecchio PJ, Keese CR, Giaever I. Electrical method for detection of endothelial cell shape change in real time: assessment of endothelial barrier function. Proc Natl Acad Sci USA. 1992; 89(17):7919–7923. [PubMed: 1518814]

Umemoto EY, Speck M, Shimoda LM, Kahue K, Sung C, Stokes AJ, Turner H. Single-walled carbon nanotube exposure induces membrane rearrangement and suppression of receptor-mediated signalling pathways in model mast cells. Toxicol Lett. 2014; 229(1):198–209. [PubMed: 24910985]

van Berlo D, Wilhelmi V, Boots AW, Hullmann M, Kuhlbusch TA, Bast A, Schins RP, Albrecht C. Apoptotic, inflammatory, and fibrogenic effects of two different types of multi-walled carbon nanotubes in mouse lung. Arch Toxicol. 2014; 88(9):1725–1737. [PubMed: 24664304]

Vittori Antisari L, Carbone S, Gatti A, Vianello G, Nannipieri P. Toxicity of metal oxide (CeO_2, Fe_3O_4, SnO_2) engineered nanoparticles on soil microbial biomass and their distribution in soil. Soil Biol Biochem. 2013; 60:87–94.

Wepasnick KA, Smith BA, Schrote KE, Wilson HK, Diegelmann SR, Fair-brother DH. Surface and structural characterization of multi-walled carbon nanotubes following different oxidative treatments. Carbon. 2011; 49(1):24–36.

Wick P, Manser P, Limbach LK, Dettlaff-Weglikowska U, Krumeich F, Roth S, Stark WJ, Bruinink A. The degree and kind of agglomeration affect carbon nanotube cytotoxicity. Toxicol Lett. 2007; 168(2):121–131. [PubMed: 17169512]

Worle-Knirsch JM, Pulskamp K, Krug HF. Oops they did it again! Carbon nanotubes hoax scientists in viability assays. Nano Lett. 2006; 6(6):1261–1268. [PubMed: 16771591]

Xiao C, Lachance B, Sunahara G, Luong JH. Assessment of cytotoxicity using electric cell–substrate impedance sensing: concentration and time response function approach. Anal Chem. 2002a; 74(22):5748–5753. [PubMed: 12463358]

Xiao C, Lachance B, Sunahara G, Luong JH. An in-depth analysis of electric cell-substrate impedance sensing to study the attachment and spreading of mammalian cells. Anal Chem. 2002b; 74(6): 1333–1339. [PubMed: 11924593]

Yashunsky V, Lirtsman V, Golosovsky M, Davidov D, Aroeti B. Real-time monitoring of epithelial cell–cell and cell–substrate interactions by infrared surface plasmon spectroscopy. Biophys J. 2010; 99(12):4028–4036. [PubMed: 21156146]

Ye S, Jiang Y, Zhang H, Wang Y, Wu Y, Hou Z, Zhang Q. Multi-walled carbon nanotubes induce apoptosis in raw 264.7 cell-derived osteoclasts through mitochondria-mediated death pathway. J Nanosci Nanotechnol. 2012; 12(3):2101–2112. [PubMed: 22755027]

Zhao Y, Lawrie JL, Beavers KR, Laibinis PE, Weiss SM. Effect of DNA induced corrosion on passivated porous silicon biosensors. ACS Appl Mater Interfaces. 2014; 6(16):13510–13519. [PubMed: 25089918]

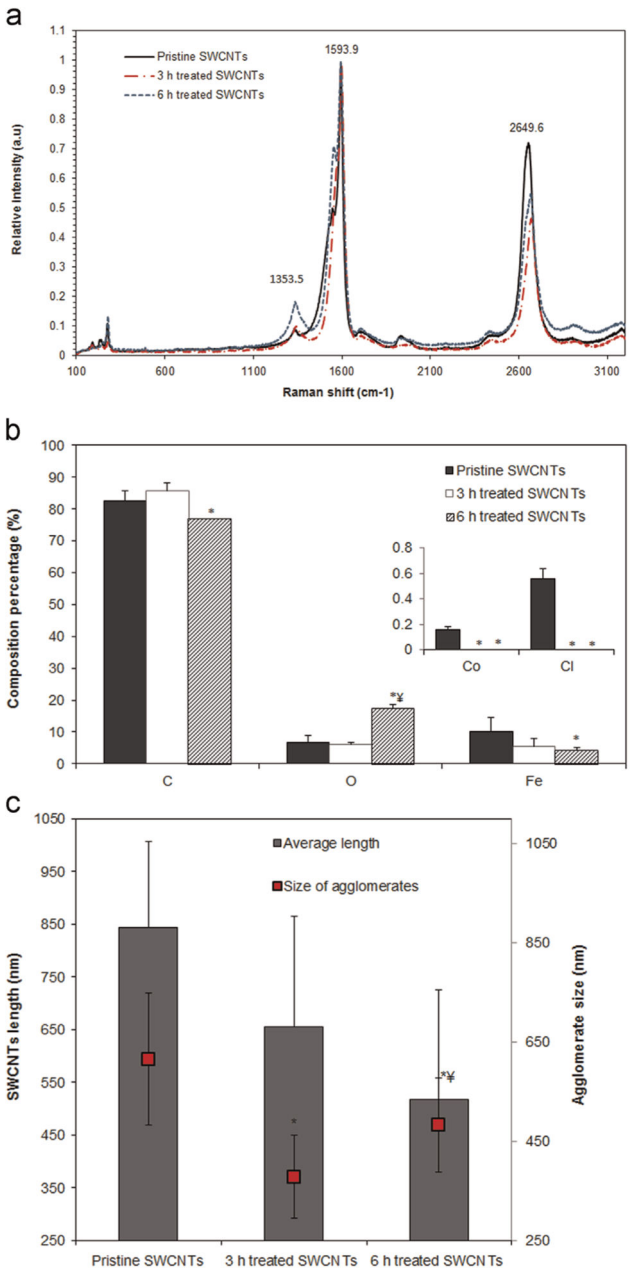

Fig. 1.

Characterization of the chemical and physical properties of the single-walled carbon nanotubes (SWCNTs) library. (a) Raman spectra. (b) Elemental composition and (c) Length and agglomerate size analyzes as a function of the treatment time. (* indicates a significant difference between the pristine and acid treated SWCNTs, while ¥ indicates a significant difference between the 3 and 6 h treated SWCNTs respectively, $p<0.05$).

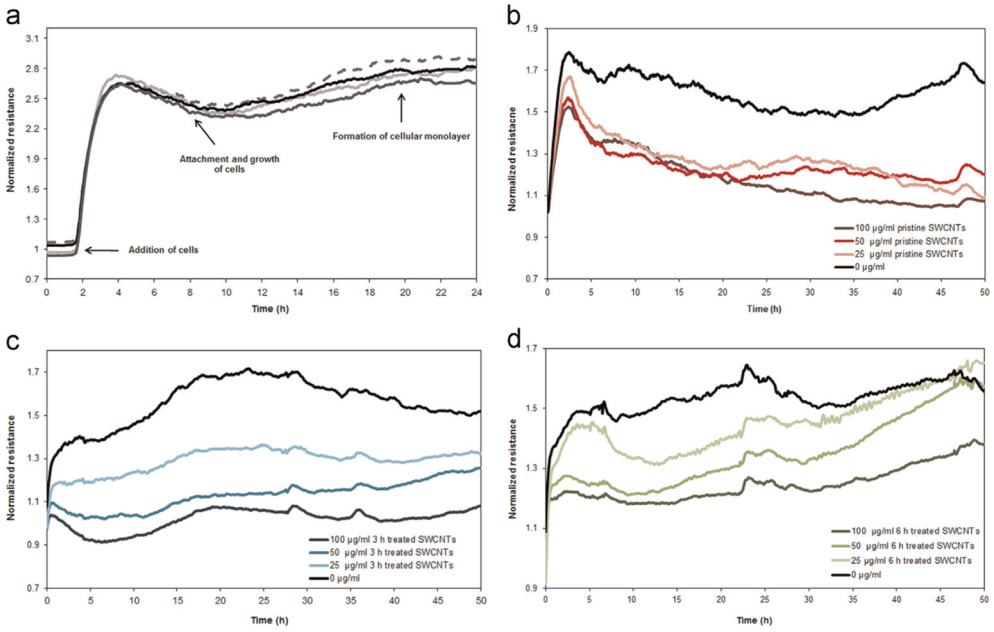

Fig. 2.

Representative real-time measurements of the normalized resistance showing changes in the cellular behavior from inoculation until the formation of a confluent monolayer (4 replicates of the cells are being shown) (a), and subsequently 48 h following exposure to (b) Pristine, (c) 3 and (d) 6h treated SWCNTs.

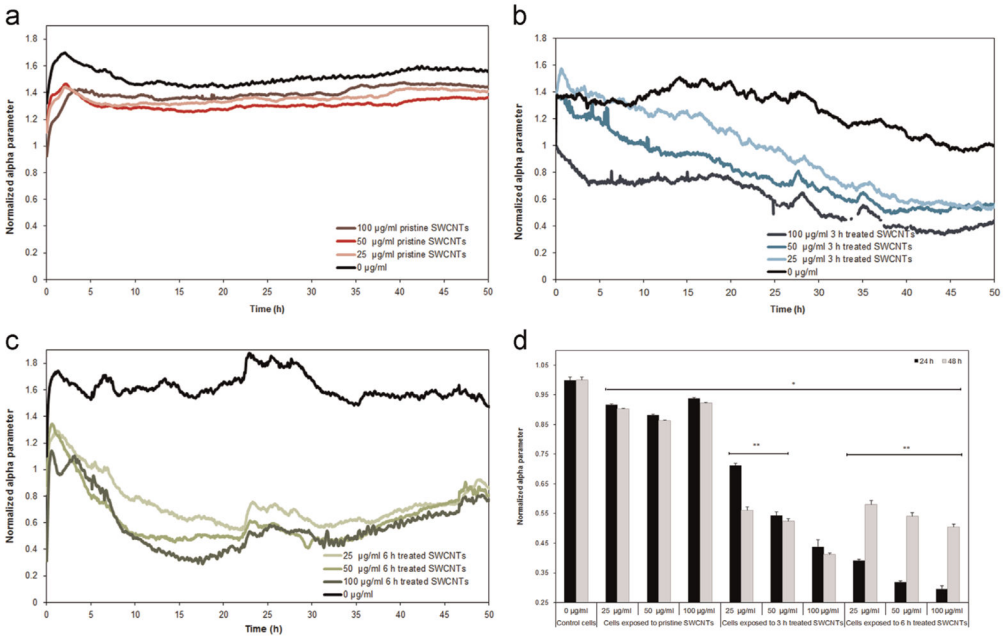

Fig. 3.

Real-time measurements of the normalized alpha parameter following exposure to (a) Pristine, (b) 3 and (c) 6 h treated SWCNTs for 48 h. (d) Cross-comparison of alpha parameter following 24 and 48 h exposure to the different SWCNTs samples. (* indicates significant differences between the alpha values for the cells exposed to SWCNTs and control cells; ** indicates significant differences between the alpha values after 24 and 48 h of exposure, $p<0.05$).

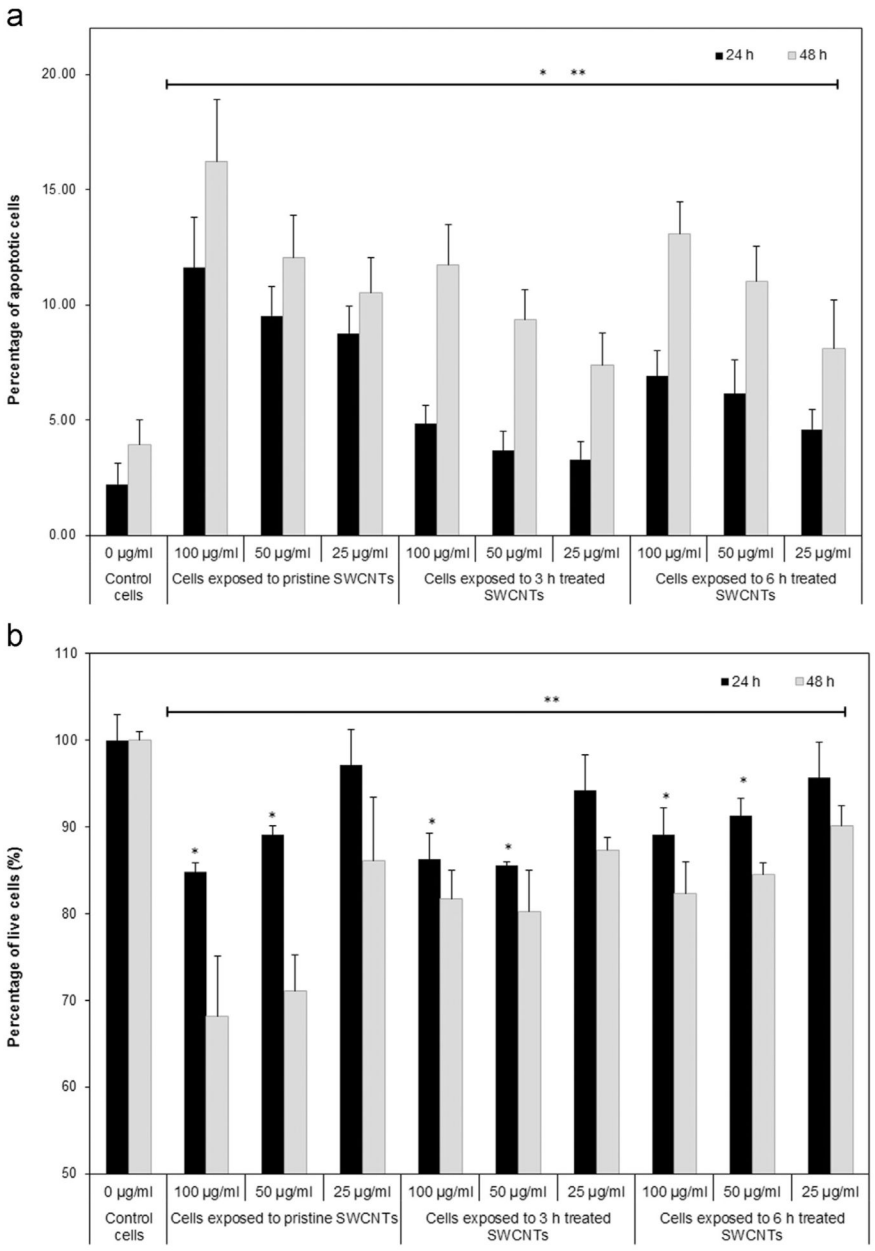

Fig. 4.

Analyzes of cellular viability following exposure to different doses of pristine, 3 and 6 h treated SWCNTs for 24 and 48 h respectively. (a) Percentage of apoptotic cells, and (b) Percentage of live cells relative to control cells. (* and ** indicate significant differences between SWCNTs-exposed cells and control cells after 24 and 48 h respectively, $p<0.05$).

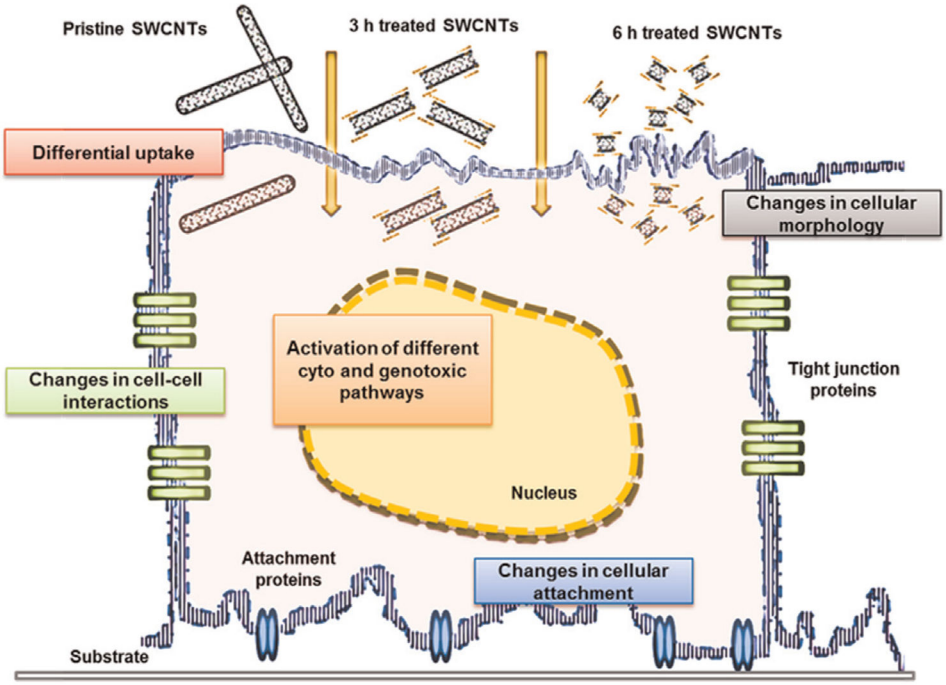

Fig. 5.

Schematic of the SWCNT-induced cellular changes as reflected by changes in cellular morphology, cell–cell interactions, and cellular attachment properties. Those changes were interpreted in relation to the SWCNT's physicochemical characteristics to reflect how nanotube internalization changes cellular fate.